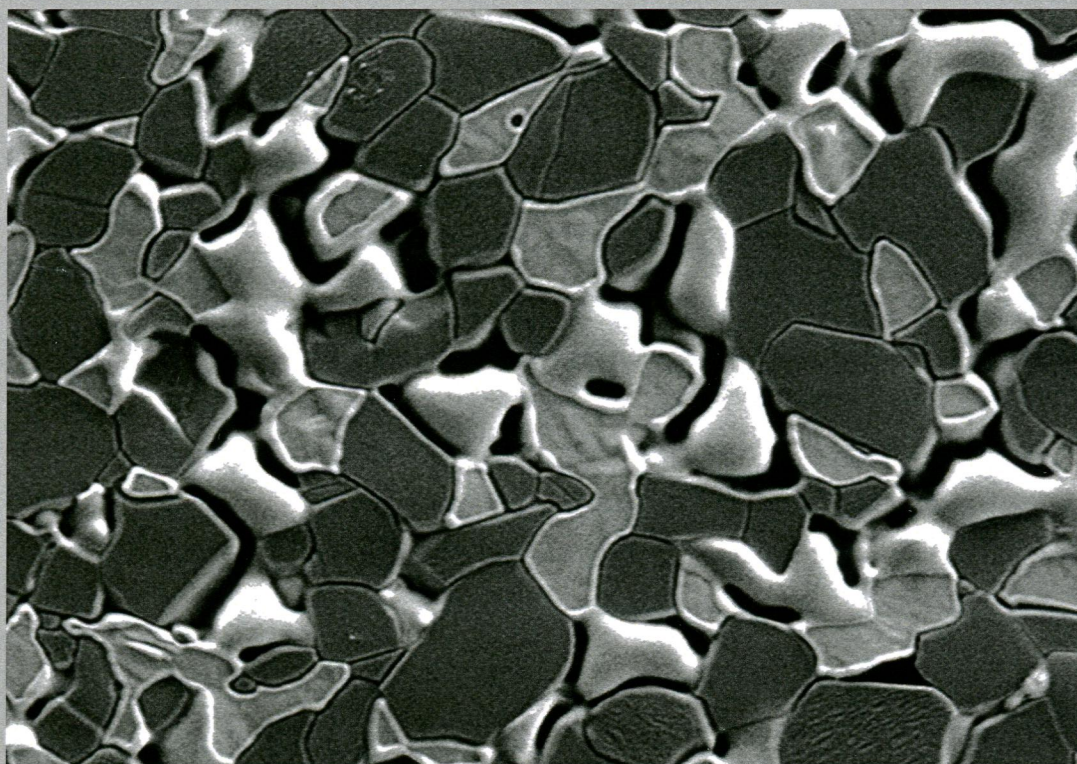




Journal of Nuclear Materials



EDITORS

- L.K. MANSUR — Oak Ridge, TN, USA (Chairman)
M. GRIFFITHS — Chalk River, ON, Canada
T. MUROGA — Toki, Japan
T. OGAWA — Niigata, Japan
R.E. STOLLER — Oak Ridge, TN, USA
L.O. WERME — Uppsala, Sweden

Abstracted/Indexed in: Aluminium Industry Abstracts/Chemical Abstracts/Current Contents: Engineering, Computing and Technology/Current Contents: Physical, Chemical and Earth Sciences/El Compendex Plus/Engineered Materials Abstracts/Engineering Index/INSPEC/Metals Abstracts. Also covered in the abstract and citation database Scopus®. Full text available on ScienceDirect®

CONTENTS

Microstructural investigation of Si-ion-irradiated single crystal 3C-SiC and SA-Tyrannohex SiC fiber-bonded composite at high temperatures, C.-Y. Ho, S.-C. Tsai, H.-T. Lin, F.-R. Chen and J.-J. Kai		Removal of deuterium from carbon-based codeposits by hydrogen isotope exchange, T.J. Finlay, J.W. Davis and A.A. Haasz	145
Thermal fatigue damage of Cu–Cr–Zr alloys, A. Chatterjee, R. Mitra, A.K. Chakraborty, C. Rotti and K.K. Ray	1	Constitutive modeling for the anisotropic uniaxial ratcheting behavior of Zircaloy-4 alloy at room temperature, H. Li, M. Wen, G. Chen, W. Yu and X. Chen	152
A thermodynamic model of thermal end elastic properties of curium, A.A. Povzner, A.N. Filanovich and V.A. Oskina	8	Oxidation studies of Fe10CrAl–RE alloys exposed to Pb at 550 °C for 10,000 h, J. Ejenstam, M. Halvarsson, J. Weidow, B. Jönsson and P. Szakalos	161
Influence of temperature on corrosion rate and porosity of corrosion products of carbon steel in anoxic bentonite environment, J. Stouřil, J. Kaňok, M. Kouřil, H. Parschová and P. Novák	17	Flux effect analysis in WWER-440 reactor pressure vessel steels, A. Kryukov, D. Blagoeva and L. Debarberis	171
The effect of gamma ray irradiation on PAN-based intermediate modulus carbon fibers, B. Li, Y. Feng, G. Qian, J. Zhang, Z. Zhuang and X. Wang	20	Separate effects identification via casting process modeling for experimental measurement of U–Pu–Zr alloys, J. Crapps, D.S. DeCroix, J.D. Galloway, D.A. Korzekwa, R. Aikin, R. Fielding, R. Kennedy and C. Unal	176
High temperature reaction between sea salt deposit and (U,Zr)O ₂ simulated corium debris, M. Takano and T. Nishi	26	Hydrogen permeability through beryllium films and the impact of surface oxides, B. Zajec, V. Nemanić, M. Žumer, C. Porosnicu and C.P. Lungu	185
The discrepancies in multistep damage evolution of yttria-stabilized zirconia irradiated with different ions, T. Yang, C.A. Taylor, S. Kong, C. Wang, Y. Zhang, X. Huang, J. Xue, S. Yan and Y. Wang	32	First-principles investigations of the physical properties of binary uranium silicide alloys, J. Yang, J. Long, L. Yang and D. Li	195
Microstructural evolution of CANDU spacer material Inconel X-750 under in situ ion irradiation, H.K. Zhang, Z. Yao, C. Judge and M. Griffiths	40	Corrosion behavior of 9Cr-ODS steel in stagnant liquid lithium and lead–lithium at 873 K, Y. Li, H. Abe, T. Nagasaka, T. Muroga and M. Kondo	200
Hot-rolling of reduced activation 8CrODS ferritic steel, X. Wu, S. Ukai, B. Leng, N. Oono, S. Hayashi, H. Sakasegawa and H. Tanigawa	49	Studies on the interaction of hydrogen with Li ₂ TiO ₃ pebbles and pellets, S. Kumar, A. Mukherjee, S. Sonak and N. Krishnamurthy	207
Cascade defect evolution processes: Comparison of atomistic methods, H. Xu, R.E. Stoller and Y.N. Osetsky	59	Effect of ion irradiation on the thermal conductivity of UO ₂ and U ₃ O ₈ epitaxial layers, P.B. Weisensee, J.P. Feser and D.G. Cahill	212
In situ TEM observation of dislocation evolution in Kr-irradiated UO ₂ single crystal, L.-F. He, M. Gupta, C.A. Yablinsky, J. Gan, M.A. Kirk, X.-M. Bai, J. Pakarinen and T.R. Allen	66	Thermophysical properties of BaUO ₄ , K. Tanaka, K. Tokushima, K. Kurosaki, Y. Ohishi, H. Muta and S. Yamanaka	218
Diffusion bonding of the oxide dispersion strengthened steel PM2000, W. Sittel, W.W. Basuki and J. Aktaa	71	Semiconducting behavior and bandgap energies of oxide films grown on alloy 600 under PWR simulated primary water conditions with different dissolved hydrogen contents, A. Loucif, J.-P. Petit and Y. Wouters	222
Assessment of structures and stabilities of defect clusters and surface energies predicted by nine interatomic potentials for UO ₂ , S.A. Taller and X.-M. Bai	78	Kinetic model for quartz and spinel dissolution during melting of high-level-waste glass batch, R. Pokorný, J.A. Rice, J.V. Crum, M.J. Schweiger and P. Hrma	230
Investigation on electronic, mechanical and thermal properties of Hf–H system, H. Wang and K. Konashi	84	Formation of (Cr,Al)UO ₄ from doped UO ₂ and its influence on partition of soluble fission products, M.W.D. Cooper, D.J. Gregg, Y. Zhang, G.J. Thorogood, G.R. Lumpkin, R.W. Grimes and S.C. Middleburgh	236
X-ray diffraction study on microstructures of shot/laser-peened AISI316 stainless steel, M. Kumagai, K. Akita, Y. Itano, M. Imafuku and S.-i. Ohya	99	Elevated temperature tensile properties of P9 steel towards ferritic steel wrapper development for sodium cooled fast reactors, B.K. Choudhary, M.D. Mathew, E.I. Samuel, J. Christopher and T. Jayakumar	242
Microstructure and mechanical property of ferritic–martensitic steel cladding under a 650 °C liquid sodium environment, J.H. Kim and S.H. Kim	107	Removal of uranium (VI) from aqueous systems by nanoscale zero-valent iron particles suspended in carboxy-methyl cellulose, I.-C. Popescu (Hoștuc), P. Filip, D. Humelnicu, I. Humelnicu, T.B. Scott and R.A. Crane	250
Radiation damage in multiphase ceramics, D. Men, M.K. Patel, I.O. Usov, M. Toïammou, I. Monnet, J.C. Pivin, J.R. Porter and M.L. Mecartney	112	Ferritic oxide dispersion strengthened alloys by spark plasma sintering, K.N. Allahar, J. Burns, B. Jaques, Y.Q. Wu, I. Charit, J. Cole and D.P. Butt	256
Spatially resolved stochastic cluster dynamics for radiation damage evolution in nanostructured metals, A.Y. Dunn, L. Capolungo, E. Martínez and M. Cherkaoui	120		
Structure and properties of calcium iron phosphate glasses, B. Qian, X. Liang, C. Wang and S. Yang	128		
	140		

(Contents continued on inside back cover)



Effect of neutron irradiation on the microstructure of the stainless steel electrosag weld overlay cladding of nuclear reactor pressure vessels, <i>T. Takeuchi, Y. Kakubo, Y. Matsukawa, Y. Nozawa, Y. Nagai, Y. Nishiyama, J. Katsuyama, K. Onizawa and M. Suzuki</i>	266	The incorporation of plutonium in lanthanum zirconate pyrochlore, <i>D.J. Gregg, Y. Zhang, S.C. Middleburgh, S.D. Conradson, G. Triani, G.R. Lumpkin and E.R. Vance</i>	444
Simulation of the nanostructure evolution under irradiation in Fe-C alloys, <i>V. Jansson and L. Malerba</i>	274	Observations of orientation dependence of surface morphology in tungsten implanted by low energy and high flux D plasma, <i>H.Y. Xu, Y.B. Zhang, Y. Yuan, B.Q. Fu, A. Godfrey, G. De Temmerman, W. Liu and X. Huang</i>	452
Thermal diffusivity measurement of (U, Pu)O _{2-x} at high temperatures up to 2190 K, <i>K. Morimoto, M. Kato and M. Ogasawara</i>	286	High-temperature stability of laser-joined silicon carbide components, <i>M. Herrmann, W. Lippmann and A. Hurtado</i>	458
H ₂ O ₂ and radiation induced dissolution of UO ₂ and SIMFUEL in HCO ₃ ⁻ deficient aqueous solution, <i>S. Sundin, B. Dahlgren, O. Roth and M. Jonsson</i>	291	Studies on sintering kinetics of ThO ₂ -UO ₂ pellets using master sintering curve approach, <i>J. Banerjee, A. Ray, A. Kumar and S. Banerjee</i>	467
Application of pulsed laser irradiation for removal of hydrogen retained in tungsten, <i>K. Hirata, K. Furumoto, N. Yamamoto and T. Tanabe</i>	298	Influence of thermal aging on microstructure and mechanical properties of CLAM steel, <i>L. Huang, X. Hu, C. Yang, W. Yan, F. Xiao, Y. Shan and K. Yang</i>	479
Influence of grain size on radiation effects in a low carbon steel, <i>A. Alsabbagh, R.Z. Valiev and K.L. Murty</i>	302	Creep deformation and mechanisms in Haynes 230 at 800 °C and 900 °C, <i>G.J. Pataky, H. Sehitoglu and H.J. Maier</i>	484
Influence of gamma ray irradiation on metakaolin based sodium geopolymer, <i>D. Lambertin, C. Boher, A. Dannoux-Papin, K. Galliez, A. Rooses and F. Frizon</i>	311	Characterization of self-damaged (U,Pu)N fuel used in the NIMPHE program, <i>U. Carvajal-Nunez, D. Prieur, A. Janssen, T. Wiss, A. Cambriani, E. Vermorel, A. Scheinost and J. Somers</i>	491
Hydrogen isotope effect on storage behavior of U ₂ Ti and UZr _{2,3} , <i>R.A. Jat, S.G. Sawant, M.B. Rajan, J.R. Dhanuskar, S. Kaity and S.C. Parida</i>	316	Thermal shock behaviour of tungsten after high flux H-plasma loading, <i>M. Wirtz, J. Linke, G. Pintsuk, G. De Temmerman and G.M. Wright</i>	497
Review of PWSCC and mitigation management strategies of Alloy 600 materials of PWRs, <i>S.S. Hwang</i>	321	Hydrogen solubility in zirconium intermetallic second phase particles, <i>P.A. Burr, S.T. Murphy, S.C. Lumley, M.R. Wenman and R.W. Grimes</i>	502
Thermodynamic modeling of the U-Zr system – A revisit, <i>W. Xiong, W. Xie, C. Shen and D. Morgan</i>	331	HLW glass dissolution in the presence of magnesium carbonate: Diffusion cell experiment and coupled modeling of diffusion and geochemical interactions, <i>M. Debure, L. De Windt, P. Frugier and S. Gin</i>	507
Thermal conductivity of UO _{2+x} and U ₄ O _{9-y} , <i>J.T. White and A.T. Nelson</i>	342	Neutron and X-ray diffraction analysis of the effect of irradiation dose and temperature on microstructure of irradiated HT-9 steel, <i>P.L. Mosbrucker, D.W. Brown, O. Anderoglu, L. Balogh, S.A. Maloy, T.A. Sisneros, J. Almer, E.F. Tulk, W. Morgenroth and A.C. Dippel</i>	522
Alloying effect of Ni and Cr on irradiated microstructural evolution of type 304 stainless steels, <i>L. Tan and J.T. Busby</i>	351	Multidimensional multiphysics simulation of TRISO particle fuel, <i>J.D. Hales, R.L. Williamson, S.R. Novascone, D.M. Perez, B.W. Spencer and G. Pastore</i>	531
Molecular dynamics simulation of dislocations in uranium dioxide, <i>P. Fossati, L. Van Brutzel and B. Devincere</i>	359	Helium mobility in SON68 borosilicate nuclear glass: A nuclear reaction analysis approach, <i>R. Bès, T. Sauvage, S. Peugeot, J. Haussy, F. Chamssedine, E. Oliviero, T. Fares and L. Vincent</i>	544
Effect of orientation on plastic deformations of Alloy 617 for VHTR applications, <i>K. Mo, G. Lovicu, H.-M. Tung, X. Chen, Y. Miao, J.B. Hansen and J.F. Stubbins</i>	366	Adsorption of H atoms on cubic Er ₂ O ₃ (001) surface: A DFT study, <i>W. Mao, T. Chikada, K. Shimura, A. Suzuki, K. Yamaguchi and T. Terai</i>	555
Concomitant formation of different nature clusters and hardening in reactor pressure vessel steels irradiated by heavy ions, <i>K. Fujii, K. Fukuya and T. Hojo</i>	378	Study of temperature and radiation induced microstructural changes in Xe-implanted UO ₂ by TEM, STEM, SIMS and positron spectroscopy, <i>N. Djourelov, B. Marchand, H. Marinov, N. Moncoffre, Y. Pipon, N. Béreid, P. Nédélec, L. Raimbault and T. Epicier</i>	562
Impact of long-term thermal exposure on a SiC fiber-reinforced copper matrix composite, <i>S. Kimmig, S. Elgeti and J.-H. You</i>	386	An efficient numerical method for intergranular fission gas evolution under transient with piecewise boundary resolution, <i>Y. Cui, S. Ding, Y. Huo, C. Wang and L. Yang</i>	570
Efficiency of generation of optical centers in KS-4V and KU-1 quartz glasses at neutron and gamma irradiation, <i>A.Kh. Islamov, U.S. Salikhbaev, E.M. Ibragimova, I. Nuritdinov, B.S. Fayzullaev, K.Yu. Vukolov and I. Orlovskiy</i>	393	Multiphysics modeling of porous CRUD deposits in nuclear reactors, <i>M.P. Short, D. Hussey, B.K. Kendrick, T.M. Besmann, C.R. Stanek and S. Yip</i>	579
The thermal performance of fuel matrix material in a CO ₂ atmosphere, <i>J.D. Turner, M.J.S. Schmidt and T.J. Abram</i>	398	Thermochemical modeling of the U _{1-y} Gd _y O _{2±x} phase, <i>J.W. McMurray, D. Shin, B.W. Slone and T.M. Besmann</i>	588
Numerical simulation of the bubble growth due to hydrogen isotopes inventory processes in plasma-irradiated tungsten, <i>C. Sang, J. Sun, X. Bonnin, S. Liu and D. Wang</i>	403	Evaluation of sintering effects on SiC-incorporated UO ₂ kernels under Ar and Ar-4% ³ H ₂ environments, <i>C.M. Silva, T.B. Lindemer, R.D. Hunt, J.L. Collins, K.A. Terrani and L.L. Snead</i>	596
TEM study of beryllium pebbles after neutron irradiation up to 3000 appm helium production, <i>M. Klimenkov, V. Chakin, A. Moeslang and R. Rolli</i>	409	Long-term corrosion behavior of CVD SiC in 360 °C water and 400 °C steam, <i>J.-Y. Park, I.-H. Kim, Y.-I. Jung, H.-G. Kim, D.-J. Park and W.-J. Kim</i>	603
Crystal growth and thermoluminescence response of NaZr ₂ (PO ₄) ₃ at high gamma radiation doses, <i>E. Ordóñez-Regil, A. Contreras-Ramírez, S.M. Fernández-Valverde, P.R. González-Martínez and H. Carrasco-Ábrego</i>	424	Oxygen diffusion in niobia-doped zirconia as surrogate for oxide film on Zr-Nb alloy: AC impedance analysis, <i>T. Yamana, T. Arima, T. Yoshihara, Y. Inagaki and K. Idemitsu</i>	608
Incorporation of cerium in zirconolite-sphene Synroc, <i>S. Wang, Y. Teng, L. Wu, K. Zhang, X. Ren, H. Yang and L. Xu</i>	432		
Immobilization of simulated radioactive soil waste containing cerium by self-propagating high-temperature synthesis, <i>X. Mao, Z. Qin, X. Yuan, C. Wang, X. Cai, W. Zhao, K. Zhao, P. Yang and X. Fan</i>	436		
Thermodynamic investigation on MTe ₂ O ₆ (M = Th, Ce), <i>A. Jain, R. Pankajavalli and S. Anthonysamy</i>			
An investigation of the oxidation behaviour of zirconium alloys using isotopic tracers and high resolution SIMS, <i>S.S. Yardley, K.L. Moore, N. Ni, J.F. Wei, S. Lyon, M. Preuss, S. Lozano-Perez and C.R.M. Grovenor</i>			